AGU PUBLICATIONS

Geophysical Research Letters

RESEARCH LETTER
10.1002/2015GL064521

Key Points:
- Trends in SAM are within the natural variability of CMIP5 models
- Jet magnitude and location trends are outside natural variability of models
- There are differences in trends between SAM, jet location, and jet magnitude

Correspondence to:
J. L. Thomas,
jthom143@jhu.edu

Citation:
Thomas, J. L., D. W. Waugh, and A. Gnanadesikan (2015), Southern Hemisphere extratropical circulation: Recent trends and natural variability, *Geophys. Res. Lett.*, *42*, doi:10.1002/2015GL064521.

Received 20 MAY 2015
Accepted 4 JUN 2015
Accepted article online 6 JUN 2015

Southern Hemisphere extratropical circulation: Recent trends and natural variability

Jordan L. Thomas[1], Darryn W. Waugh[1], and Anand Gnanadesikan[1]

[1]Department of Earth and Planetary Sciences, Johns Hopkins University, Baltimore, Maryland, USA

Abstract Changes in the Southern Annular Mode (SAM), Southern Hemisphere (SH) westerly jet location, and magnitude are linked with changes in ocean circulation along with ocean heat and carbon uptake. Recent trends have been observed in these fields but not much is known about the natural variability. Here we aim to quantify the natural variability of the SH extratropical circulation by using Coupled Model Intercomparison Project Phase 5 (CMIP5) preindustrial control model runs and compare with the observed trends in SAM, jet magnitude, and jet location. We show that trends in SAM are due partly to external forcing but are not outside the natural variability as described by these models. Trends in jet location and magnitude, however, lie outside the unforced natural variability but can be explained by a combination of natural variability and the ensemble mean forced trend. These results indicate that trends in these three diagnostics cannot be used interchangeably.

1. Introduction

The Southern Ocean plays a critical role in the ocean overturning circulation and moderating global climate through carbon and heat uptake [*Khatiwala et al.*, 2009; *Gnanadesikan*, 1999], with approximately 40% of anthropogenic carbon and 75% of heat entering the ocean south of 30°S [*Frölicher et al.*, 2015; *Sabine et al.*, 2004]. The leading mode of Southern Hemisphere (SH) extratropical variability, the Southern Annular Mode (SAM), has been shown to directly affect this overturning circulation and the distribution of anthropogenic carbon uptake by altering the magnitude and location of the westerly jet [*Hall and Visbeck*, 2002; *Mignone et al.*, 2006; *Sen Gupta and England*, 2006]. It is therefore important to understand the variability in the SH extratropical circulation.

Observations and reanalyses have shown a positive trend in SAM and jet magnitude over the last couple of decades along with a poleward shift in the jet location [*Thompson et al.*, 2000; *Thompson and Solomon*, 2002] in addition to trends in subtropical sea surface temperature, Antarctic sea ice extent, ocean ventilation, and gyre circulation [*Parkinson and Cavalieri*, 2012; *Swart and Fyfe*, 2012; *Waugh et al.*, 2013; *Roemmich et al.*, 2007]. Additionally, studies have detected anthropogenic influences in surface pressure and the westerly jet [*Gillett et al.*, 2003, 2005]. These trends in the SAM and consequently the jet have been largely attributed to ozone depletion in the SH stratosphere during austral summer [*Previdi and Polvani*, 2014; *Gillett et al.*, 2013; *Gillett and Thompson*, 2003]. However, there is also evidence that this positive phase trend in the SAM is due in part to greenhouse gas warming [*Arblaster and Meehl*, 2006; *Lee and Feldstein*, 2013; *Gillett et al.*, 2013].

While there is evidence of anthropogenic forcing, understanding the forcing in the context of natural variability is difficult given the lack of in situ observations and satellite information prior to 1979. Previous studies have tried to quantify the natural variability in the SH using proxy records [*Marshall*, 2003; *Visbeck*, 2009] and climate models [*Latif et al.*, 2013]. Understanding the relative contribution of natural variability and anthropogenic forcing to recent trends is critical to understanding how global climate will be influenced in the future.

In this study, we aim to further estimate the natural variability of the SH extratropical circulation by using the Coupled Model Intercomparison Project Phase 5 (CMIP5) preindustrial control model runs. We examine five metrics of the SH extratropical circulation: the SAM, the jet location defined using the 850 mb winds (U_{lat}) and the surface wind stress (τ_{lat}), the jet magnitude defined by the 850 mb winds (U_{max}), and the surface wind stress (τ_{max}). We turn to CMIP5 preindustrial model runs to quantify the natural variability of these five metrics to address the following questions: Can recently observed trends in SH circulation occur in CMIP5 piControl model runs due to natural variability alone, do the CMIP5 models historical (1980–2004) runs show significant

Table 1. CMIP5 Models Used in This Study

Model	piControl Model Run Length (years)	Historical Model Ensemble Runs
CanESM2	996	1
CNRM CM5	850	10
GFDL ESM2M	500	1
IPSL CM5a LR	1000	6
IPSL CM5a MR	300	3
IPSL CM5b LR	300	1
MIROC ESM	531	3
MIROC ESM CHEM	255	1
MIROC5	200	5
MPI ESM LR	1000	3
MPI ESM MR	1000	3
MRI CGCM3	500	3
NOR ESM1m M	501	1
NOR ESM1m ME	252	1

trends in the circulation metrics, and do these simulated historical trends capture the characteristics of the observed trends?

2. Methods

In order to examine the natural multidecadal-scale variability in the SH circulation, we use a combination of preindustrial control ("piControl") and historical (1980 to 2004) runs from models. Table 1 lists the models used in this study, the length of their piControl run, and the number of historical runs. The models were chosen based on the availability of monthly mean fields of sea level pressure, 850 mb zonal winds, and zonal wind stress for both piControl and historical runs. We focused on the austral summer (averaged over December, January, and February) because this is the season where the largest trends are observed [*Thompson and Solomon*, 2002; *Thompson et al.*, 2011].

From the monthly sea level pressure, we calculated the SAM as the zonal sea level pressure difference between 65° and 40° South. For the sake of comparisons across different models, we chose to leave the SAM as a surface pressure difference as opposed to normalizing by the standard deviation as done in *Gong and Wang* [1999] to avoid normalizing by different standard deviations across models. Additionally, we examine the SH westerly jet magnitude and location calculated using both zonal surface wind stress (τ_{max} and τ_{lat}) and 850 mb zonal winds (U_{max} and U_{lat}). To find the jet maximum and location, the maximum zonal mean wind stress/850 mb winds and the surrounding four grid points were isolated and interpolated to a 0.1° meridional grid. A quadratic polynomial was then fit to the interpolated data, and the maximum magnitude and location were found.

While there are no trends (i.e., drift) in these metrics over the length of the piControl time series (order 250–1000 years), strong multidecadal trends are found. Time series in SAM from a high-varying model (MPI ESM MR) and a low-varying model (MIROC5) are shown in Figures 1a and 1c, respectively. As highlighted in red, there are multiple 25 year periods that have strong trends even though there is no trend over the entire time series. In order to quantify the variability of these multidecadal-scale trends, we calculate the linear trend of each metric (SAM, τ_{max}, τ_{lat}, U_{max}, and U_{lat}) for consecutive and overlapping 25 year trends for each model's piControl run (*Polvani and Smith*, [2013] performed a similar analysis for sea ice extent in piControl runs).

We focus on the period 1980–2004 because reanalyses are unreliable before the implementation of satellites in 1979 [*Swart and Fyfe*, 2012] (Figure 1). Our analysis goes up until 2004 in order to compare with the CMIP5 historical model runs, which are typically run until year 2005. To verify that period length does not influence our results, the same analysis with CMIP5 piControl model runs and observations for the 34 year period between 1980 and 2014 was conducted (not shown). The results are essentially identical to those reported below as the observed changes over this period are either the same size or smaller than over the 1980–2005 period, and the modeled trends are only slightly smaller.

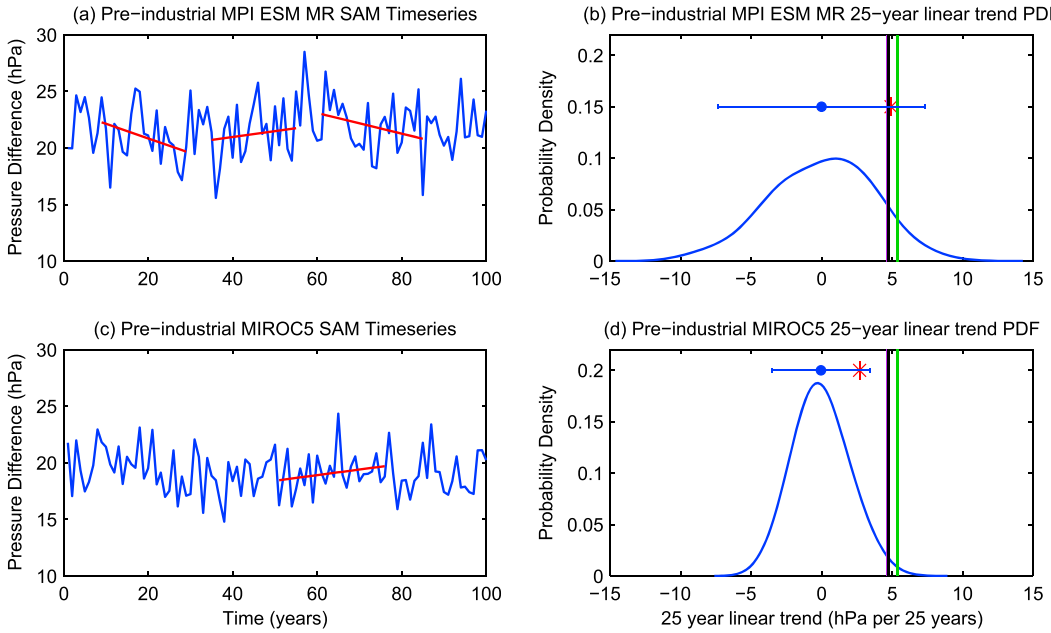

Figure 1. SAM time series for (a) MPI ESM MR and (c) MIROC5 piControl runs over the first 100 years. The red lines indicate periods where the trend is greater than the average reanalysis trend between 1980 and 2004. (b and d) The probability density functions for the 25 year linear SAM trends in MPI ESM MR and MIROC5, respectively. The blue dot represents the mean of the 25 year trends, while the whiskers extend 2 standard deviations. The vertical lines represent the observed trends: National Centers for Environmental Prediction (NCEP) R1 (green), NCEP R2, ERA-Interim, and JRA-55 (black), and the red asterisk shows the magnitude of the historical model run trend (first ensemble member).

The distribution of these 25 year trends for the model piControl run is a measure of the natural multidecadal variability in each model (in other words, the model internal variability with no anthropogenic influences). As an example, the probability density function of these 25 year linear trends for the MPI ESM MR and MIROC5 models is shown in Figures 1b and 1d. The blue curve shows the probability density of the 25 year linear trends for the SAM, and the whisker plot shows the mean (blue circle) and 2 standard deviations (whisker extent) of the 25 year trends. The means of the 25 year trends (blue dot) are near zero, consistent with there being no drift in the piControl runs, but the trend for any individual 25 year period varies from −10 to +10 hPa per 25 years (with standard deviation of around 4 hPa per 25 years). Throughout the rest of the paper, we shall use the whiskers to represent the distribution of 25 year trends from the model piControl runs. Each CMIP5 model has a different piControl run length, which could potentially impact our model-model comparisons. However, subsampling the output from 1000 year piControl runs shows limited sensitivity of the standard deviation of 25 year trends for run lengths between 250 and 1000 years.

To compare the observations with the modeled natural variability, we used four reanalysis products: NCEP Reanalysis 1 (NCEP-1) [*Kalnay et al.*, 1996], NCEP Reanalysis 2 (NCEP-2) [*Kanamitsu et al.*, 2002], ERA-Interim [*Dee et al.*, 2011], and JRA-55 [*Kobayashi et al.*, 2015] during the period 1980–2004. We also calculated the linear trend between the years 1980 and 2004 from the model historical runs and compared both with the observed trends and model natural decadal variability. The vertical lines in Figures 1b and 1d represent the 1980–2004 reanalysis trends, and the red asterisk shows historical simulation trend.

3. Results and Discussion

3.1. Natural Variability

We first examine the distribution of 25 year linear trends from CMIP5 piControl runs. Figure 2 shows, as whisker plots, the distributions of 25 year linear trends of (a) SAM, (b) U_{lat}, (c) τ_{lat}, (d) U_{max}, and (e) τ_{max} for each model. For all five metrics, the mean 25 year linear trend (blue circles) is around zero for all the models, as expected for unforced model runs with no drift. The width of the whiskers is, however, variable across the different models, indicating differences in the multidecadal variability among the models. Models with larger whiskers are more variable with stronger multidecadal trends than models with smaller whiskers.

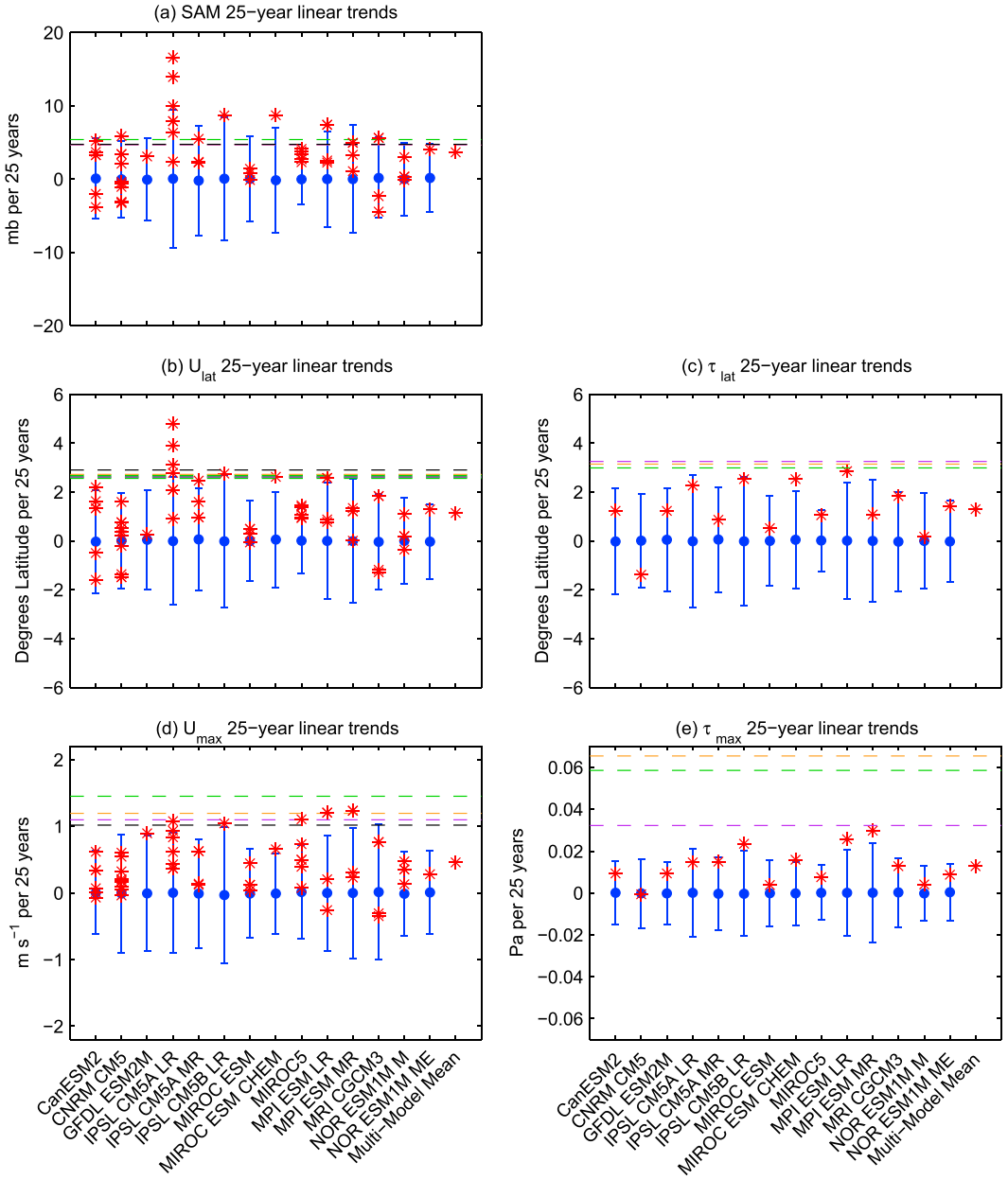

Figure 2. Natural variability, historical trends, and observations for (a) SAM, (b) 850 mb jet latitude, (c) wind stress jet latitude, (d) 850 mb jet magnitude, and (e) wind stress jet magnitude. Blue circles show the mean of the piControl 25 year linear trends indicating model drift. Whisker length is 2 standard deviations. Red points show the historical run trends for each ensemble member. Horizontal dashed lines indicate the absolute value of the observed trends: NCEP R1 (green), NCEP R2 (orange), ERA-Interim (purple), and JRA-55 (black).

The variability of the whisker width among the models differs among the five metrics. The SAM (Figure 2a) shows the most variability among the models, with the width of the whiskers ranging from 3 hPa per 25 years to 10 hPa per 25 years (the mean and 2 sigma of the whisker length for the ensemble of models is 6 ± 3 hPa per 25 years). This indicates there is little agreement in the magnitude of the natural variability of the unforced system in SAM among the CMIP5 models. The jet location variability, U_{lat} (Figure 2b) and τ_{lat} (Figure 2c), also differs across the various models, but the differences are not as pronounced as in the SAM (whisker width is 2 ± 0.75° per 25 years). There is even less variability between the models in jet magnitude. For the 850 mb winds (Figure 2d), the whisker extent is 0.75 ± 0.25 m s^{-1} per 25 years, while for magnitude of the surface wind stress (Figure 2e) it is approximately 0.015 ± 0.005 Pa per 25 years. To better understand how these metrics compare to each other, we compare the linear correlations of each of the jet metrics with the SAM (Figure 3).

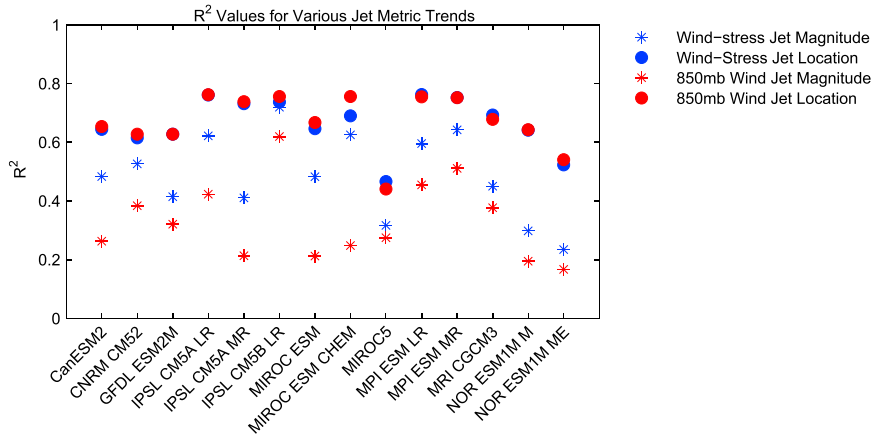

Figure 3. Correlation coefficient squared for correlation of the 25 year linear trends in wind stress jet location, wind stress jet magnitude, 850 mb jet location, and 850 mb jet magnitude with the 25 year trends in SAM for each model.

The highest correlations occur between the SAM and the jet latitude metrics, with average R^2 values of 0.7 for both τ_{lat} and U_{lat}. The correlations between the SAM and jet magnitude metrics are significantly lower with average R^2 values at 0.5, with the R^2 values for correlations of SAM with τ_{max} always being greater than that of SAM with U_{max}.

The comparison of magnitude of natural decadal variability of the different metrics and correlation between the metrics shows our first key result: The SAM, jet location, and jet magnitude metrics are not interchangeable.

3.2. Observed Trends

With a description of the natural variability from the piControl run for each model, we now compare the observed reanalysis trends to the modeled natural variability to examine if the observed trend is forced or natural. In each panel in Figure 2, the dashed horizontal lines show the magnitude of the observed reanalysis trends. As expected from the above analysis, there are differences among the different metrics.

The observed SAM trend observations lie just within the whiskers for most of the models, indicating the observed trends lie within the model natural variability. To quantify this further, the probability of each model randomly obtaining a trend with the magnitude of the average reanalysis SAM trend or larger is shown in Table 2 (column 1). Ten of the 14 models have a probability of 5% or greater, and thus there is a significant (at the 5% level) probability of obtaining the observed 25 year trend in the piControl simulations by chance alone. In other words, the observed trend over the period 1980–2004 in the SAM lies just within the edge of natural variability as described by these models. This result also holds for the period 1980–2014 (not shown).

The observed τ_{lat} and U_{lat} trends are just outside the model's natural decadal variability (Figures 2b and 2c). If we calculate the probability of each model obtaining the observed average reanalysis U_{lat} trend (Table 2, column 2), then we see that no models have a probability of 5% or greater; however, 6 of the 14 have greater than a 1% probability. Thus, there is not a significant (at the 5% level) probability of obtaining the observed trend using natural variability alone.

In contrast, the observed trends in τ_{max} and U_{max} are both outside the natural variability as described by the models (Figures 2d and 2e). The probability of obtaining the average reanalysis U_{max} trend in all but one of the piControl models is less than 1% (Table 2, column 3); and therefore, there is not a significant (at the 1% level) probability of the natural variability reproducing the observed trend. The probabilities of the piControl τ_{max} and τ_{lat} obtaining the observed trends are not shown in Table 2 but are consistent with the U_{max} and U_{lat} probabilities.

The above shows that the observed trends in the SAM largely lie at the edge of natural multidecadal variability of the piControl model runs. However, this does not necessarily mean that the observed trends are not forced by anthropogenic activities, merely that the observations can contain a large component of natural variability in the SAM. The observed trend in the jet location and magnitude, however, is outside the variability of most

Table 2. Probability of Obtaining Averaged Reanalysis Trend by Only Natural Variability (First Three Columns) and Natural Variability + Historical Multimodel Ensemble Trend (Second Three Columns)[a]

	Natural Variability			Natural Variability + Historical Ensemble		
Model	SAM	U_{loc}	U_{max}	SAM	U_{loc}	U_{max}
CanESM2	**5.98**%	0.09%	0.03%	**35.4**%	**9.77**%	1.77%
CNRM CM5	4.18 %	0.21%	0.28%	**34.2**%	**6.45**%	**6.71**%
GFDL ESM2M	**5.41**%	1.05%	0.71%	**32.1**%	**7.32**%	**6.92**%
IPSL CM5a LR	**17.24**%	2.79%	0.31%	**39.5**%	**13.0**%	**5.54**%
IPSL CM5a MR	**9.29**%	1.84 %	0.30%	**33.0**%	**7.31**%	4.70%
IPSL CM5b LR	**16.3**%	3.70 %	1.49%	**39.8**%	**15.3**%	**9.56**%
MIROC ESM	**5.69**%	0.078%	0.032%	**37.8**%	3.80%	2.36 %
MIROC ESM CHEM	**10.24**%	0.52%	0.044%	**34.4**%	**7.27**%	1.78%
MIROC5	1.18%	0.005%	0.36%	**26.7**%	2.13%	3.65 %
MPI ESM LR	**8.40**%	1.70%	0.81%	**34.8** %	**10.4**%	**6.67**%
MPI ESM MR	**9.50**%	1.81%	0.71%	**40.3**%	**12.3**%	**7.61**%
MRI CGCM3	**5.14**%	0.27%	0.93%	**37.0**%	**7.24**%	**9.33**%
NOR ESM1m M	3.98 %	0.09 %	0.05%	**32.6**%	**5.30**%	1.70 %
NOR ESM1m ME	3.63%	0.09%	0.04%	**33.3**%	4.46%	2.98 %

[a]Values in boldface indicate a probability of 5% or higher.

models piControl runs. This does suggest an external force driving the jet to strengthen and shift over this 25 year period.

3.3. Model Historical Trends

We now examine the model historical runs to understand how the modeled trends compare to the modeled natural variability and to compare the modeled trends with the observed trends. The red asterisks in Figure 2 represent the 25 year trend for each historical run (the number of historical runs varies among the models).

There is considerable variability among the models in the magnitude of the trends, but for all five metrics the vast majority of the simulated historical trends are of the same sign (increase in SAM, poleward shift, and strengthening of the jet). This consistency in sign indicates that external (anthropogenic) forcing is causing at least part of the trend. However, the magnitude of the historical trends are almost all within the natural multidecadal variability of the corresponding model (i.e., within the whiskers). Thus, while the response in the models between 1980 and 2004 is due (at least in part) to forcing, the response does not overwhelm the natural variability.

For the SAM, the magnitude of the individual historical ensemble member trends is largely within the estimated natural variability and highly variable, with some ensemble members having trends of the opposite sign to the observations (dashed horizontal lines). Because the observed trends are generally within the natural decadal variability of the models, a close agreement between individual historical ensemble members and observed trends would not be expected due to the high component of natural variability. Most of the ensemble members have positive trends, and the magnitude of the multimodel ensemble mean historical trend is similar to the observations. This further suggests an anthropogenic forcing pushing the SAM toward positive phase.

The same comparison for jet location and magnitude yields different results. The observed trends in the jet metrics are outside the natural variability of the models and generally larger than the modeled historical trends (especially for the magnitude of the wind stress). A possible cause for this is that the observed trends are due to anthropogenic forcing that is not well represented (or underrepresented) in the models. However, another possibility is that there are issues with the reanalyses, and the reanalyses are overestimating the real trend. This may especially be the case for the NCEP reanalyses, where the wind stress trends are significantly outside the model natural variability but the 850 hPa winds are just outside the model natural variability.

If we consider the observed trends to be a combination of natural variability and external forcing, and if we use the ensemble mean historical trend as a representation of the forced response, we can better capture the

observed trend. The last three columns in Table 2 show the probability of obtaining the mean reanalysis trend from a combination of each model's natural variability and the multimodel ensemble mean historical trend (results for τ_{lat} and τ_{max} are not shown, but are consistent with U_{lat} and U_{max}). The probabilities for each metric are substantially greater, indicating that there is a significant probability, in most models, that the observed trends are due to this combination of natural variability and anthropogenic forcing. This does not exclude the possibility that the models are systematically biased low, or that the reanalyses are biased high, but it suggests that the mismatch is smaller than might be suggested from previous work [*Swart and Fyfe*, 2012].

4. Conclusions

Changes in the SAM are often linked with concurrent changes in the SH westerly jet magnitude and location [*Hall and Visbeck*, 2002]. Additionally, observational studies have shown recent trends in these diagnostics and attribute them to a combination of ozone depletion and greenhouse gas induced warming [*Arblaster and Meehl*, 2006]. By comparing CMIP5 models piControl and historical runs with reanalysis observations, we have shown that there are significant differences in the observed and modeled trends of the SAM from those in the jet. Hence, the SAM and jet metrics cannot be used interchangeably.

Examining the natural variability of the SAM using CMIP5 preindustrial control runs has led to the conclusion that the observed trend is not decisively outside the natural variability as simulated by the CMIP5 models. While the modeled natural variability in SAM is quite large, the positive bias of the model historical trends suggests influence of an external forcing. The failure of individual historical models to simulate the magnitude of the observed historical trend could be due to the natural variability and not deficiencies in the simulations.

In contrast, the observed trends in jet location and magnitude are outside the natural variability of the models. The historical model runs also seem to underestimate the magnitude of these trends, especially in jet magnitude. Combining the natural variability and historical trend brings the models closer to capturing the observed trends in jet location and magnitude, but this does not eliminate the possibility that the model trends are biased low or the reanalyses are biased high.

Changes in the SAM and SH westerly jet have been linked with significant changes in ocean circulation, ocean heat and carbon uptake [*Mignone et al.*, 2006], and Antarctic sea ice extent [*Fan et al.*, 2014]. We suggest that changes in SAM and jet latitude may behave differently than changes in jet magnitude and thus may have independent effects on the Southern Ocean and Antarctic climate. Understanding how these atmospheric variables interact with each other will be critical for predicting the future evolution of ocean circulation and the Earth system.

Acknowledgments

This research was supported by the U.S. National Science Foundation (NSF) under grants ANT-1043307 and FESD-1338814. We thank the World Climate Research Programmes Working Group on Coupled Modelling for making the CMIP5 data available (available at *http://cmip-pcmdi.llnl.gov/cmip5/*), in addition to the modeling groups who produced this data. Reanalysis data can be found at the following websites: Reanalysis 1 *http://www.esrl.noaa.gov/psd/data/gridded/data.ncep.reanalysis.html*, Reanalysis 2 *http://www.esrl.noaa.gov/psd/data/gridded/data.ncep.reanalysis2.html*, ERA-Interim *http://apps.ecmwf.int/datasets/data/interim-full-moda/*, and JRA-55 *http://rda.ucar.edu/datasets/ds628.0/*. We would like to also thank Lorenzo Polvani and Karen Smith for their help with the CMIP5 data acquisition and helpful discussions.

The Editor thanks two anonymous reviewers for their assistance in evaluating this paper.

References

Arblaster, J. M., and G. A. Meehl (2006), Contributions of external forcings to Southern Annular Mode trends, *J. Clim.*, *19*, 2896–2905.

Dee, D. P., et al. (2011), The ERA-Interim reanalysis: Configuration and performance of the data assimilation system, *Q. J. R. Meteorol. Soc.*, *137*(656), 553–597, doi:10.1002/qj.828.

Fan, T., C. Deser, and D. P. Schneider (2014), Recent Antarctic sea ice trends in the context of Southern Ocean surface climate variations since 1950, *Geophys. Res. Lett.*, *41*, 2419–2426, doi:10.1002/(ISSN)1944-8007.

Frölicher, T. L., J. L. Sarmiento, D. J. Paynter, J. P. Dunne, J. P. Krasting, and M. Winton (2015), Dominance of the Southern Ocean in anthropogenic carbon and heat uptake in CMIP5 models, *J. Clim.*, *28*, 862–886, doi:10.1175/JCLI-D-14-00117.1.

Gillett, N. P. (2005), Detection of external influence on sea level pressure with a multi-model ensemble, *Geophys. Res. Lett.*, *32*, L19714, doi:10.1029/2005GL023640.

Gillett, N. P., and D. W. J. Thompson (2003), Simulation of recent Southern Hemisphere climate change, *Science*, *302*(5643), 273–275, doi:10.1126/science.1087440.

Gillett, N. P., F. W. Zwiers, A. J. Weaver, and P. A. Stott (2003), Detection of human influence on sea-level pressure, *Nature*, *422*(6929), 292–294.

Gillett, N. P., J. C. Fyfe, and D. E. Parker (2013), Attribution of observed sea level pressure trends to greenhouse gas, aerosol, and ozone changes, *Geophys. Res. Lett.*, *40*(10), 2302–2306, doi:10.1002/grl.50500.

Gnanadesikan, A. (1999), A simple predictive model for the structure of the oceanic pycnocline, *Science*, *283*, 2077–2079.

Gong, D., and S. Wang (1999), Definition of the Antarctic oscillation index, *Geophys. Res. Lett.*, *26*, 459–462, doi:10.1029/1999GL900003.

Hall, A., and M. Visbeck (2002), Synchronous variability in the Southern Hemisphere atmosphere, sea ice, and ocean resulting from the annular mode, *J. Clim.*, *15*, 3043–3057.

Kalnay, E., et al. (1996), The NCEP/NCAR 40-year reanalysis project, *Bull. Am. Meteorol. Soc.*, *77*, 437–471.

Kanamitsu, M., W. Ebisuzaki, J. Woollen, S.-K. Yang, J. J. Hnilo, M. Fiorino, and G. L. Potter (2002), NCEP-DOE-AMIP-II Reanalysis (R-2), *Bull. Am. Meteorol. Soc.*, *83*(11), 1631–1643, doi:10.1175/BAMS-83-11-1631.

Khatiwala, S., F. Primeau, and T. Hall (2009), Reconstruction of the history of anthropogenic CO_2 concentrations in the ocean, *Nature*, *462*(7271), 346–349, doi:10.1038/nature08526.

Kobayashi, S., Y. Ota, and Y. Hatada (2015), The JRA-55 reanalysis: General specifications and basic characteristics, *J. Meteorol. Soc. Jpn.*, *93*(1), 5–48, doi:10.2151/jmsj.2015-001.

Latif, M., T. Martin, and W. Park (2013), Southern Ocean sector centennial climate variability and recent decadal trends, *J. Clim.*, *26*(19), 7767–7782.

Lee, S., and S. B. Feldstein (2013), Detecting ozone- and Greenhouse gas-driven wind trends with observational data, *Science*, *339*(6119), 563–567, doi:10.1126/science.1225154.

Marshall, G. J. (2003), Trends in the Southern Annular Mode from observations and reanalyses, *J. Clim.*, *16*(24), 4134–4143.

Mignone, B. K., A. Gnanadesikan, J. L. Sarmiento, and R. D. Slater (2006), Central role of Southern Hemisphere winds and eddies in modulating the oceanic uptake of anthropogenic carbon, *Geophys. Res. Lett.*, *33*, L01604, doi:10.1029/2005GL024464.

Parkinson, C. L., and D. J. Cavalieri (2012), Antarctic sea ice variability and trends, 1979-2010, *Cryosphere*, *6*(4), 871–880, doi:10.5194/tc-6-871-2012.

Polvani, L. M., and K. L. Smith (2013), Can natural variability explain observed Antarctic sea ice trends? New modeling evidence from CMIP5, *Geophys. Res. Lett.*, *40*(12), 3195–3199, doi:10.1002/grl.50578.

Previdi, M., and L. M. Polvani (2014), Climate system response to stratospheric ozone depletion and recovery, *Q. J. R. Meteorol. Soc.*, *140*(685), 2401–2419, doi:10.1002/qj.2330.

Roemmich, D., J. Gilson, R. Davis, P. Sutton, S. Wijffels, and S. Riser (2007), Decadal spinup of the South Pacific subtropical gyre, *J. Phys. Oceanogr.*, *37*(2), 162–173, doi:10.1175/JPO3004.1.

Sabine, C. L., et al. (2004), The oceanic sink for anthropogenic CO_2, *Science*, *305*, 367–371, doi:10.1126/science.1097403.

Sen Gupta, A., and M. H. England (2006), Coupled ocean-atmosphere-ice response to variations in the Southern Annular Mode, *J. Clim.*, *19*(18), 4457–4486.

Swart, N. C., and J. C. Fyfe (2012), Observed and simulated changes in the Southern Hemisphere surface westerly wind-stress, *Geophys. Res. Lett.*, *39*, L16711, doi:10.1029/2012GL052810.

Thompson, D. W. J., and S. Solomon (2002), Interpretation of recent Southern Hemisphere climate change, *Science*, *296*(5569), 895–899, doi:10.1126/science.1069270.

Thompson, D. W. J., J. M. Wallace, and G. C. Hegerl (2000), Annular modes in the extratropical circulation. Part II: Trends, *J. Clim.*, *13*, 1018–1036.

Thompson, D. W. J., S. Solomon, P. J. Kushner, M. H. England, K. M. Grise, and D. J. Karoly (2011), Signatures of the Antarctic ozone hole in Southern Hemisphere surface climate change, *Nat. Publ. Group*, *4*(11), 741–749, doi:10.1038/ngeo1296.

Visbeck, M. (2009), A station-based Southern Annular Mode index from 1884 to 2005, *J. Clim.*, *22*(4), 940–950.

Waugh, D. W., F. Primeau, T. DeVries, and M. Holzer (2013), Recent changes in the ventilation of the Southern Oceans, *Science*, *339*(6119), 568–570, doi:10.1126/science.1225411.